www.lajss.org
Latin American Journal of Solids and Structures 1 (2004) 423–441

"Dynamic plastic" and "dynamic progressive" buckling of elastic-plastic circular shells - revisited

D. Karagiozova

Institute of Mechanics, Bulgarian Academy of Sciences
Acad. G. Bonchev St., Block 4, Sofia 1113, Bulgaria

Abstract

Two typical buckling patterns of circular cylindrical shells, which can occur due to axial impact loadings, are discussed. The phenomena of "dynamic plastic" buckling (when the entire length of a cylindrical shell wrinkles before the development of large radial displacements) and "dynamic progressive" buckling (when the folds in a cylindrical shell form sequentially) are analyzed from the viewpoint of stress wave propagation resulting from an axial impact. It is shown that the particular impact velocity, which instantaneously causes stresses that exceed the elastic limit of the material at the proximal end of a shell, and therefore can cause the initial instability pattern within a sustained axial plastic flow, depends on the material properties. The present analysis reveals that "dynamic plastic" buckling can develop for relatively low impact velocity, too provided that a shell has certain inertia characteristics. The latter conclusion is in contrast with the established perception that the high impact velocity is a necessary condition for the initial shell instability within a sustained axial plastic flow. A phenomenological approach is used to predict the buckling mode of a circular shell under axial impact with a given initial velocity.

Keywords: Axial impact, plastic stress waves, circular shells, dynamic plastic buckling, progressive buckling

1 Introduction

The experimental [1-8] and some recent theoretical studies [9-15] show that the variety of the dynamic buckling responses of axially loaded shells is caused by the coupling of the inertia and inelastic material properties. In particular, the three types of instability namely "dynamic plastic" buckling (when the entire length of a cylindrical shell wrinkles before the development of large radial displacements), "dynamic progressive" buckling (when the folds in a cylindrical shell form sequentially) and global bending (when the shell buckles in an Euler mode) develop according to the geometry of the shell, loading conditions and material properties.

* Corresp. author E-mail: d.karagiozova@imbm.bas.bg Received 30 Oct 2004; In revised form 14 Nov 2004

Notation

c, c_p	speed of the elastic and plastic stress wave in a circular shell, respectively
D, h, L	outer diameter, thickness and length of a circular shell, respectively
E, E_h	Young's modulus and strain hardening modulus, respectively
G	striking mass
l	length of a single axisymmetric wrinkle, Eq. (3)
l_s	length of a single axisymmetric wrinkle, Eq. (4)
ρh	mass per unit circumferential length of a single wrinkle, Fig. 6
t_1	duration of the compression phase
T_0	initial impact energy
V_0	impact velocity
V_1	vertical velocity of a shell predicted by the discrete model, Figs. 4 and 6
$V_{1,str}$	velocity of the striking mass
w	radial displacement at the tip of an axisymmetric wrinkle
δ	overall reduction of the length of a single axisymmetric wrinkle due to compression without buckling, Fig. 6
ε_x, ϵ_θ, ϵ_e	axial, circumferential and equivalent strains in a circular shell, respectively
σ_0, σ_e	yield stress and equivalent stress, respectively
σ_x, σ_θ	stresses in a circular shell in the axial and circumferential direction

The transition between the global bending and progressive buckling has an important implication on the load carrying capacity of a shell so that it is important to identify the factors causing the transition between these types of buckling. The major factors for the transition between the progressive buckling and global bending mode are discussed in details in [14] and an empirical criterion for this type of transition is proposed in [15]. While this transition has an important practical implication, the transition between the "dynamic plastic" and "dynamic progressive" buckling is interesting from the view point of the buckling phenomenon itself. Based on some experimental observations [1,2], it was originally anticipated that the high velocity impact is a necessary and sufficient condition to observe "dynamic plastic" buckling in axially loaded cylindrical shells [1, 2, 16].

Further theoretical [9-11] and experimental [3-5] studies revealed that the high impact velocity is not a sufficient condition for the development of this particular buckling pattern. It is shown that "dynamic plastic" buckling can develop only within a sustained axial plastic flow [9-11]. Factors, which cause a transition from dynamic plastic to dynamic progressive buckling for relatively high impact velocities, have been identified in [9-11] and they are closely related to the material characteristics and the inertia properties of a shell. These studies confirmed that for the range of the material parameters analysed in [1,2,9-11] (different types of aluminium alloys), the initial shell instability pattern with small wrinkles along the entire length can occur for relatively high impact velocities provided that a shell has certain inertia properties.

On the other hand, the development of the so called "dynamic plastic" buckling, has been mainly analysed for shells made from aluminium alloys [1-5,9-11,17], so that the inertia properties of the shell related to the radial displacements were varied within relatively small interval by the variation of the shell thickness. A considerable increase of the impact velocity is required in order to experimentally observe measurable wrinkles along the entire shell length due to the relatively small effect of the radial inertia on the response of an aluminium alloy shell.

The material density is another parameter that affects the inertia of a shell, therefore it is important to analyse whether shells with significantly different material characteristics, say steel shells, can respond in a similar to the aluminium alloy shells manner when subjected to axial impact loadings with different initial velocities.

The purpose of the present study is to explore the influence of the material properties, in particular the influence of the density and material strain hardening, on the patterns of axisymmetric buckling in order to establish whether the high velocity impact is a necessary condition for the development of "dynamic plastic" buckling. Any strain rate effects are neglected in the present study.

It should be noted that, in addition to above classification of buckling patterns (modes), progressive buckling of a circular shell can occur with the development of axisymmetric or asymmetric wrinkles depending on the shell geometry, material properties and loading conditions [8] but this transition is not discussed in the present article. It is assumed that, similarly to the "dynamic plastic" buckling, axisymmetric wrinkles develop in the case of progressive buckling, too.

2 Buckling within a sustained axial plastic flow

Several experimental studies on axial impact of elastic-plastic cylindrical shells show that the response of a cylindrical shell, which buckles inelastically develops in two phases: initial instability pattern dominated by an axial compression and a structural collapse when large bending deformations occur [1,2]. Recent studies reported in the literature [9-11] reveal that the initial instability pattern for elastic-plastic cylindrical shells subjected to an axial impact loading depends not only on the inertia characteristics of the shell, but is strongly influenced by the material hardening properties. It has been established [2-4,9-11] that the "dynamic progressive" buckling (Fig. 1(b-e)) dominates the shell response for a wide range of loading and material parameters [9-11] while "dynamic plastic" buckling (Fig. 1(f,g)) can develop only within the sustained axial plastic flow along the entire length of a shell during the first phase of deformation [1,9-11]. In the latter case, relatively large axial plastic strains propagate along an elastic-plastic shell due to the instantaneously applied load. Buckling develops plastically, so that no elastic unloading due to the growth of the radial displacements occurs across the shell thickness [9, 10, 17].

A comparison between the initial shell instability patterns and the final buckling shapes of a shell having a length $L = 4D$ and subjected to a 2 kJ impact applied with different initial

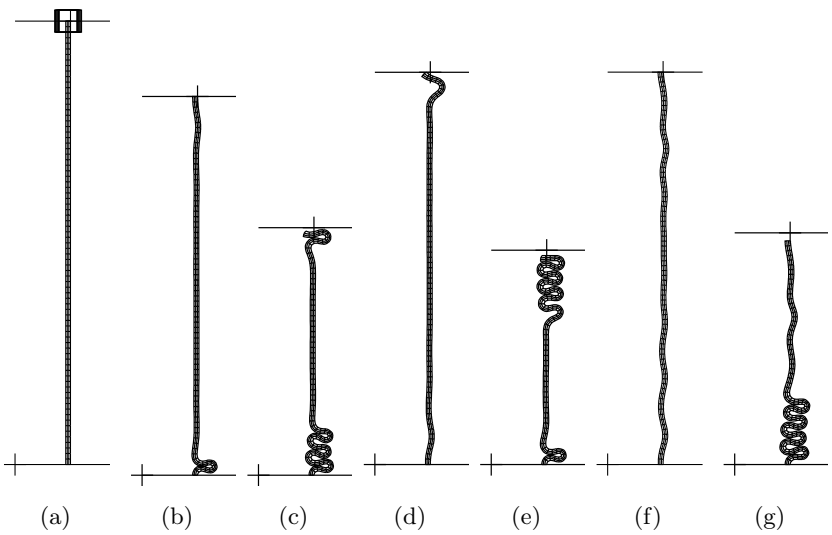


Figure 1: Distinguishing between "progressive" and "dynamic plastic" buckling, $D = 30$ mm, $h = 1.5$ mm, $\sigma_0 = 175$ MPa (only the thickness of the shell is shown). (a) Undeformed; (b,c) $V_0 = 30$ m/s, $E_h = 600$ MPa; (d,e) $V_0 = 75$ m/s, $E_h = 180$ MPa; (f,g) $V_0 = 75$ m/s, $E_h = 600$ MPa.

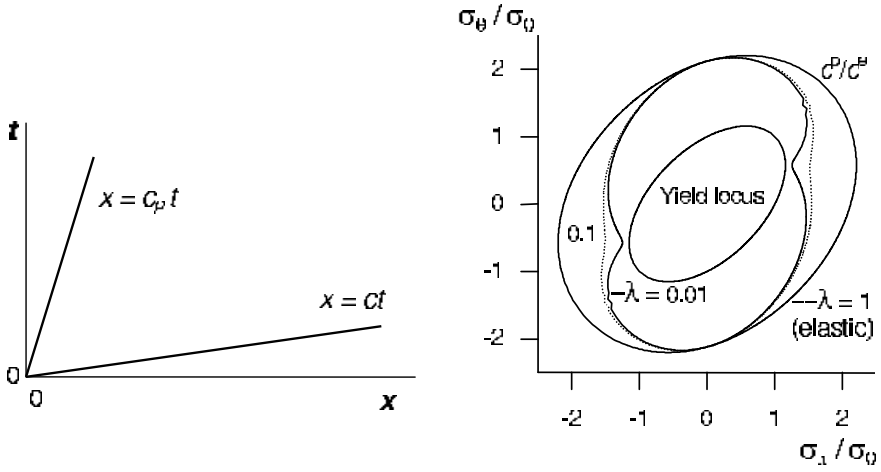
velocities is presented in (Fig. 1) for two materials with different strain hardening moduli. It is evident that the 30 m/s impact initiates "progressive" buckling while a 75 m/s impact causes wrinkles along the entire shell length (Fig. 1(f,g)). However, "progressive" buckling occurs for a 75 m/s impact, too when decreasing the material hardening modulus (Fig. 1(d,e)).

In general, dynamic progressive buckling develops in shells, which exhibit small radial inertia effects under axial loading when the radial displacements grow quickly and cause localization of large bending strains before the plastic stress wave can travel a distance along the shell length sufficient to cause the initiation of the next wrinkle. In a way of contrast, "dynamic plastic" buckling occurs when the radial inertia prevents from the rapid growth of the radial displacements, so that the plastic stress wave can travel a longer distance and eventually can cover the entire length of a shell thus causing small wrinkles along the shell. It is clear that these two typical axisymmetric buckling patterns are determined by the particular combination between the speed of the plastic stress wave (governed by the material density and strain hardening) and the inertia characteristics of a shell.

For a bilinear elastic-plastic material, the stress at the proximal end of a shell resulting from an instantaneously applied axial load at $t = 0$ (Fig. 2(a), $\lambda = E_h/E$) and exceeding the elastic limit of the material is obtained as [11]

$$\sigma^0(t=0) = 2\sigma_0/\sqrt{3} + \rho c^p_{min}(V_0 - V_{0,plastic}), \tag{1}$$

where σ_0 is the yield stress and $c^p_{min} \approx 2\left[E_h/(\rho(1-\nu^2)\right]^{1/2}/\sqrt{3}$ is the minimum speed of the



(a) (b)

Figure 2: Stress wave characteristics. (a) Characteristics of the stress wave propagation problem [10] for instantaneously applied load with an initial velocity, which causes stresses exceeding the elastic limit of the material; (b) Plastic wave speeds in an elastic-plastic medium with linear strain hardening obeying the von Mises yield criterion [10].

plastic stress wave, which occurs for the stress state ($\sigma_x < 0, \sigma_\theta = 0$) (Fig. 2(b)). This stress wave speed is characteristic of the compression phase and further in the present analysis is referred to as c_p. The impact velocity, which can initiate an instantaneous plastic stress at the proximal end of a shell depending on the yield stress, material density and the elastic wave speed is

$$V_{0,plastic} = 2\sigma_0/(\rho c\sqrt{3}). \tag{2}$$

Since the speed of the elastic stress waves, c, varies only slightly for many ductile materials, it is evident that the impact velocity, which causes instantaneous plastic stress in circular shells made from, e.g., steel having $\rho = 7800$ kg/m^3, is considerably lower than the corresponding velocity for shells made from aluminium alloy ($\rho = 2700$ kg/m^3) when assuming the same yield stress. Thus, a sustained axial plastic flow can be initiated for relatively low impact velocities in circular shells made of steel provided appropriate inertia characteristics of a shell. For example, $V_{0,plastic} = 25.1$ m/s for an aluminium alloy with $\sigma_0 = 300$ MPa, while impact velocities larger than $V_{0,plastic} = 8.74$ m/s are sufficient to initiate instantaneous plastic stress in a steel shell. It is shown in [9] that an initial shell instability in the mode of "dynamic plastic" buckling can be observed for impact velocities larger than 30 m/s, approximately while $V_{0,plastic} = 24.68$ m/s for this particular material.

The numerical simulations in the present study were carried out using the FE code ABAQUS — Standard. It is assumed that an axisymmetric buckling mode develops, so that 2D axisym-

metric solid elements CAX8 (eight nodes biquadratic) are used for the calculations. The load is applied as a point mass which is attached to the nodes of a rigid body. A constant amplitude force applied to the nodes of the rigid-body models the gravitational load. The contact between the shell and the striking mass is defined using the 'surface interaction' concept together with a friction coefficient of 0.25 in order to prevent sliding at the proximal end. Any self-contact of the inner and the outer surfaces of the shell are assumed frictionless.

The axial and the radial degrees of freedom of the nodes at the distal end are fixed in order to model a clamped end, but no constraints are assumed for the degrees of freedom associated with the nodes at the proximal end. The modelled shell has no initial imperfections. Models of an elastic-plastic materials with linear strain hardening and obeying the Mises yield criterion is used for all of the calculations.

3 A discrete model for the development of a single wrinkle - a phenomenological approach

The numerical simulations of axial impact loadings of an elastic-plastic circular shell show that although small winkles are observed along the entire length in the case of "dynamic plastic" buckling, these wrinkles develop sequentially as soon as the plastic stress wave travels a distance larger than a critical length associated with the length of a single wrinkle. For example, the approximate plateau stress, which is observed for $t = 0.1$ ms corresponds to the development of the first two axisymmetric wrinkles of a shell, while at $t = 0.144$ ms three wrinkles are observed as shown in Fig. 3. A dispersion of the axial plastic strains occurs and plastic strains with smaller magnitudes propagate further, but it can be anticipated that a "plateau" stress corresponds to the axial stress, which causes buckling. It is interesting to observe that the growth of the radial displacements associated with the current wrinkle diminishes as soon the next wrinkle starts to develop and eventually stops.

This kind of response suggests that the development of small wrinkles within the sustained axial plastic flow can be analysed when assuming that the axial velocity of the proximal end of a shell is determined by a sequential development of single wrinkles. A schematic illustration of modelling the development of an axisymmetric buckling of a shell is shown in Fig. 4. In this sketch, $\triangle(t) = t_i - t_{i-1}$ is the time for the propagation of the plastic stress wave a distance equal to the length of a wrinkle. It is anticipated that the particular length of the axisymmetric wrinkles, which can develop in a circular shell is known in advance. There are several expressions given in the literature for the length of an axisymmetric wrinkle but the one used in the present study, is [16]

$$\tilde{l} = \frac{\pi L}{2}\left(\sqrt{3} - \frac{h}{R}\frac{E_h}{\sigma^0}\right)^{-1}, l = 2\tilde{l}, \tag{3}$$

which is obtained assuming a sustained axial plastic flow and when the influence of the material properties is taken into account. The length of a wrinkle according to Eq. (3) is compared with

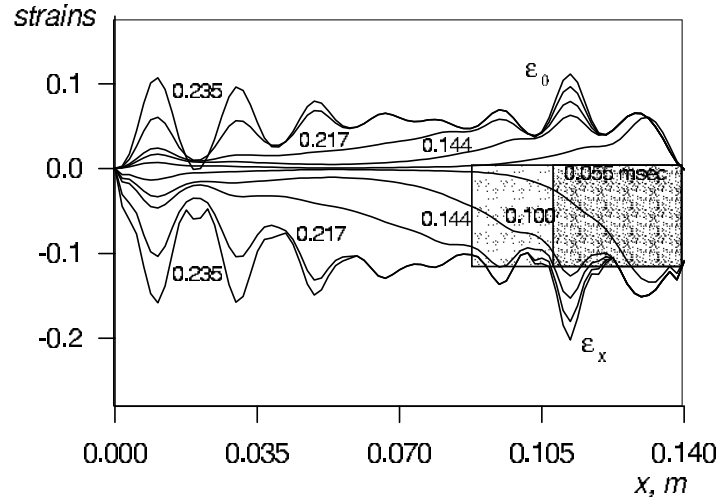


Figure 3: Distribution of the plastic strains along a shell with $D = 30$ mm, $h = 1.5$ mm, $L = 140$ mm, $\sigma_0 = 175$ MPa, $E_h = 600$ MPa, $V_0 = 75$ m/s and $G = 0.71$ kg.

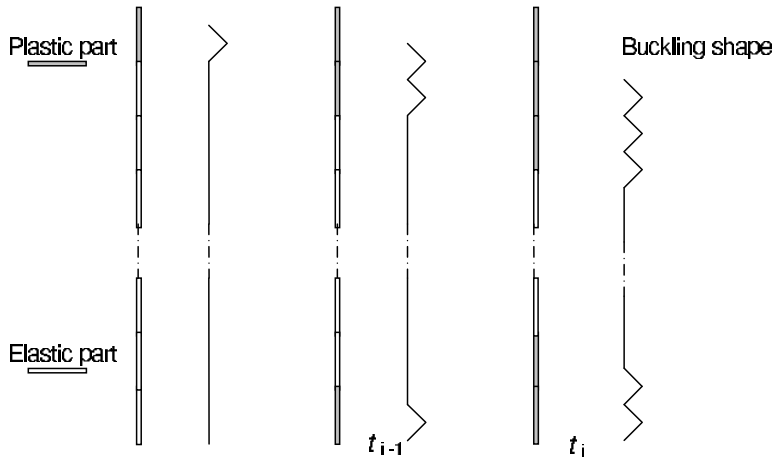


Figure 4: A sketch for the development of the buckling shape within a sustained axial plastic flow (axisymmetric mode).

the wrinkle length obtained according to another classical expression [18]

$$\tilde{l}_s = (\pi Rh/\sqrt{3})^{1/2}, l_s = 2\tilde{l}_s, \tag{4}$$

which have been mainly used for an estimation of the energy absorbing capacity of a shell when assuming progressively developed axisymmetric wrinkles.

The length of an axisymmertic wrinkle given by Eq. (4) is obtained from the energy balance and this geometric relationship has been confirmed in many experiments on axial impact of circular shell. The wrinkle length predicted by Eq. (3) can vary with the variation of the material properties of the shell, however, an axisymmetric wrinkle having an arbitrary length has no physical meaning. Therefore, the ratio $l/l_s \approx 1$ can be used to estimate the wrinkle length in an actual shell depending on the shell geometry and material properties according to Eq. (3). Figures 5(a,b) show that the length of a wrinkle depends on the hardening modulus, and this dependence is more significant for larger ratios E_h/σ_0, particularly when increasing the thickness of a shell. In these figures, l_s= 7.94 mm and 11 mm are calculated for $\sigma_0 = 100$ MPa. These results show that circular shells made from materials with relatively large ratios E_h/σ_0 can deform exhibiting asymmetric wrinkles corresponding to l/l_s larger than unity. Accordingly, the geometrical and material characteristics of the shells, which are analysed in the present study, are selected to satisfy $l/l_s \approx 1$ in order to ensure axisymmetric buckling.

A model for the initiation of a local wrinkle is shown in Fig. 6. It is assumed that the links of the model are compressible but rigid in bending. This model simplifies the initial deformation of a strip, which represents an axisymmetric wrinkle with a length according to Eq. (3) of a shell with length L. The equation of motion of the model is

$$\frac{\rho h l^3}{24}\ddot{\psi} + M_A + M_B + M_r + \frac{N_x l}{2}\psi = 0 \tag{5}$$

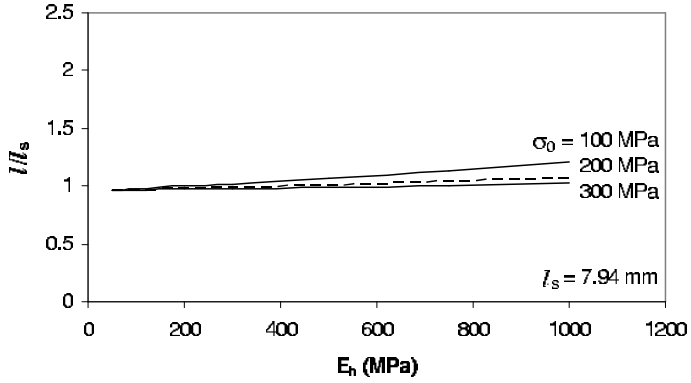
when taking into account that $M_A = M_C$ in Fig. 6. In Eq. (5), N_x is the axial force in the links, M_A and M_B are the bending moments at A and B, respectively but M_r is the bending moment resulting from the circumferential forces in an actual shell.

It is assumed that a stationary shell is struck by a mass, G, travelling with an initial velocity V_0. Buckling develops within a sustained axial plastic flow so that no elastic unloading due to the growth of the radial displacements occurs.

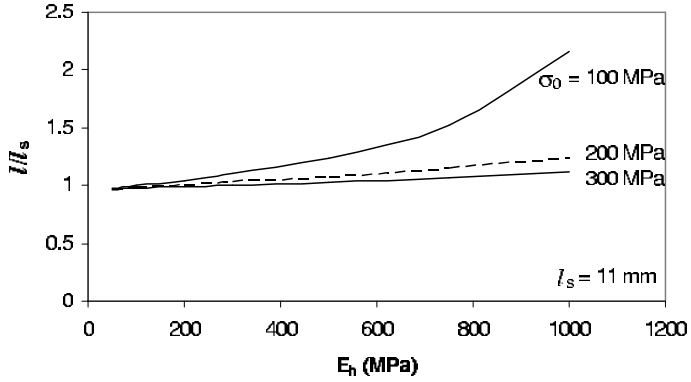
Let us consider an axisymmetric buckling of a circular shell and assume a plane stress field in the shell with $(\sigma_x < 0, \sigma_\theta \neq 0)$. According to Florence and Goodier [17], the associated total strain rates are

$$\dot{\varepsilon_x} = -\frac{V_0}{L} + z\frac{\partial^2 \dot{w}}{\partial x^2}, \dot{\varepsilon_\theta} = \left(1 - \frac{z}{R}\right)\left(\frac{V_0}{2L} - \frac{\dot{w}}{R}\right), \varepsilon_z = -\dot{\varepsilon}_x - \varepsilon_\theta, \tag{6}$$

where $z \in [-h/2, h/2]$ is the coordinate across the thickness of a shell. The stresses are defined by the Prandtl-Reuss equations with an isotropic hardening



(a)



(b)

Figure 5: Length of an axisymmetric wrinkle depending on the material properties of circular shells with $D = 25.4$ mm. (a) $h = 0.8$ mm; (b) $h = 1.65$ mm.

$$\sigma_x = \frac{2\sigma_e}{3\dot{\varepsilon_e}}\left(2\dot{\varepsilon}_x + \dot{\varepsilon}_\theta\right), \sigma_\theta = \frac{2\sigma_e}{3\dot{\varepsilon_e}}\left(2\dot{\varepsilon}_\theta + \dot{\varepsilon}_x\right), \tag{7}$$

where the equivalent stress is $\sigma_e = \sigma_0 + E_h\varepsilon_e$ and

$$\dot{\varepsilon_e} \cong \frac{V_0}{L}\left[1 + \frac{zL}{2V_0}\left(\frac{4\dot{w}}{3R^2} - 2\frac{\partial^2\dot{w}}{\partial x^2}\right)\right]. \tag{8}$$

Integrating with respect to time, the equivalent strain is

$$\varepsilon_e \cong \frac{V_0}{L}\left[t + \frac{zL}{2V_0}\left(\frac{4w}{3R^2} - 2\frac{\partial^2 w}{\partial x^2}\right)\right]. \tag{9}$$

The forces and moments acting in a shell are obtained as [16]

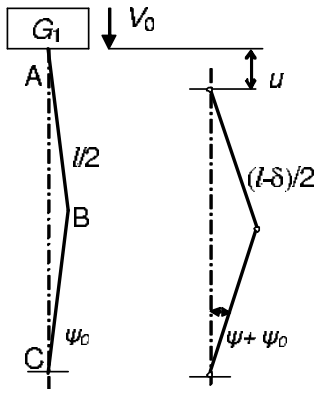


Figure 6: A discrete model for a single axisymmetric wrinkle, $G_1 = G/2\pi R$.

$$N_x = \int_{-h/2}^{h/2} \sigma_x(1 + z/R)dz = -\sigma^0 h - \frac{2\sigma^0 hL}{3V_0 R}\dot{w}, \tag{10}$$

$$\begin{aligned} M_x &= -\textstyle\int_{-h/2}^{h/2} \sigma_x(1 + z/R)zdx = \\ &= \tfrac{\sigma^0 h^3}{9R} - \tfrac{\sigma^0 h^3 L}{36V_0}\left(\tfrac{\partial^2 \dot{w}}{\partial x^2} + \tfrac{2\dot{w}}{R^2}\right) - \tfrac{h^3 E_h}{36}\left(3\tfrac{\partial^2 w}{\partial x^2} - \tfrac{2w}{R^2}\right), \end{aligned} \tag{11}$$

$$N_\theta = -\frac{4L\sigma^0 h}{3V_0 R}\dot{w}. \tag{12}$$

For small angles of rotation, $w = \tilde{l}\psi$, $\dot{w} = \tilde{l}\dot{\psi}$, and the forces and moments in the model in Fig. 6 at the different locations are

$$N_x = -\sigma^0 h, N_\theta = 0, M_x = \frac{\sigma^0 h^3}{9R} - \frac{\sigma_0 h^3 L\dot{\psi}}{36V_0\tilde{l}} - \frac{h^3 E_h \psi}{12\tilde{l}} \tag{13}$$

at A and C,

$$\begin{aligned} &N_x = -\sigma^0 h - \tfrac{2\sigma^0 hL\tilde{l}}{3V_0 R}\dot{\psi}, N_\theta = -\tfrac{4L\sigma^0 h\tilde{l}}{3V_0 R}\dot{\psi}, \\ &M_x = \tfrac{\sigma^0 h^3}{9R} + \tfrac{2\sigma_0 h^3 L\tilde{l}\dot{\psi}}{36V_0}\left(\tfrac{1}{\tilde{l}^2} - \tfrac{1}{R^2}\right) + \tfrac{2h^3\tilde{l}E_h\psi}{36}\left(\tfrac{3}{\tilde{l}^2} + \tfrac{1}{R^2}\right) \end{aligned} \tag{14}$$

at B. The projection of the circumferential forces in the direction perpendicular to the mid-surface of the shell gives rise to a force $N_\theta cos\psi/R$, which contributes to the bending moment at B as

$$M_r = -\int_0^{\tilde{l}} N_\theta x/Rdx = \frac{4L\sigma^0 h\tilde{l}^3}{9V_0 R^2}\dot{\psi} \tag{15}$$

when assuming a linear approximation for $\dot{w}(x) = 2\dot{w}_{x=\tilde{l}}x/\tilde{l}$. In an actual shell, however, the distribution of could be approximated with a non-linear function as well, e.g. quadratic or cubic one. In that case

$$M_r = -\int_0^{\tilde{l}} N_\theta x/R dx = \frac{4L\sigma^0 h\tilde{l}^3}{3V_0R^2(n+2)}\dot{\psi}, \tag{16}$$

where $n \geq 1$ is the polynomial order. Taking into account that $2\tilde{l} = l$, the equation of motion (5) becomes

$$\begin{array}{l}\ddot{\psi} + \frac{4\sigma^0 L}{\rho R^2 l^2 V_0}\left[\frac{l^2}{n+2} + \frac{h^2(2R^2-l^2)}{6l^2} - Rl\psi\right]\dot{\psi} - \\ -\frac{12\sigma^0}{\rho l^2}\left[1 - \frac{h^2 E_h(3+l^2/(2R^2))}{9\sigma^0 l^2}\right]\psi + \frac{16\sigma^0 h^2}{3\rho l^3 R} = 0.\end{array} \tag{17}$$

and the initial conditions are

$$\psi(0) = 0, \dot{\psi}(0) = V_0R/(lL) \tag{18}$$

using the relation $\dot{\varepsilon_\theta}(0) = \dot{w}/R$.

The displacement of the proximal end of the model in Fig. 6 is

$$u = (\psi^2 - \psi_0^2)l/2 + \delta, \tag{19}$$

where δ is the overall reduction of the length of the links (Fig. 6) due to their compressibility and therefore, the corresponding velocity is

$$V = \dot{u} = \psi\dot{\psi}l + \dot{\delta} = V_1 + \dot{\delta}. \tag{20}$$

The velocity due to the rotation of the links of the model in Fig. 6 is

$$V_1 = \dot{u} = \psi\dot{\psi}l. \tag{21}$$

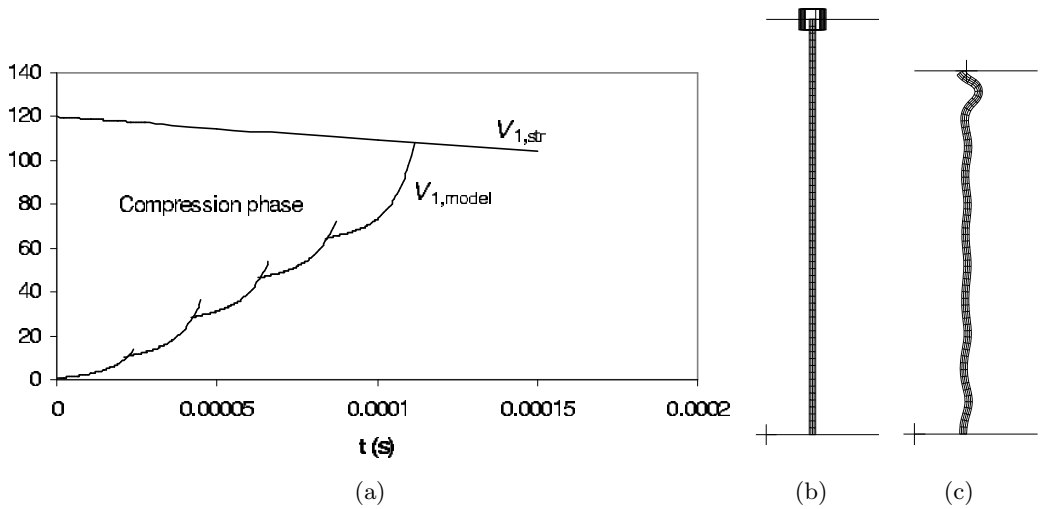
The velocity of the striker is

$$V_{1,str} = V_0 - \frac{A\sigma^0}{G}t, \tag{22}$$

where σ^0 is the stress at the proximal end of a shell at $t = 0$ due to the instantaneously initiated plastic stress according to Eq. (1). The duration of the compression phase in a shell seizes at $t = t_1$ when

$$V_{1,str}(t_1) = V_{1,model}(t_1) \tag{23}$$

where



(a) (b) (c)

Figure 7: Compression phase in an aluminium alloy shell with $D = 25.4$ mm, $h = 1.65$ mm, $\sigma_0 = 295$ MPa, $E_h = 546$ MPa, $V_0 = 120$ m/s and $G = 0.4$ kg. (a) Model prediction for the compression phase; (b) Undeformed shape; (c) Buckling shape at $t = 0.14$ ms.

$$V_{1,model} = \sum_{i=1}^{m} V_{1,i}, m \leq L/(2l). \tag{24}$$

Velocities $V_{1,i}$ are determined within intervals $t \in (t_i - t_{i-1})$ (Fig. 4) and are associated with the axial velocity due to the rotations of the links of the model in Fig. 6 according to Eq. (21), $(t_i - t_{i-1}) = l/c_p$.

An example for the duration of the compression phase of a shell struck by a mass G= 0.4 kg with $V_0 = 120$ m/s is shown in Fig. 7(a). Velocity $V_{1,model}$ is obtained from Eq. (24) when using Runge-Kutta method to integrate Eq. (17). In this figure, each "kink" corresponds to the initiation of the development of a new axisymmetric wrinkle. Depending on the impact velocity, length of the shell and speed of the plastic stress waves, winkles can develop almost simultaneously from both ends of a shell [9,10], which is the case for the the particular example shown in Fig. 7. The numerically obtained time for the onset of the bending phase is 0.135 ms, which is comparable with 0.12 ms predicted by the discrete model. The deformed shape is shown in Fig. 7(c) where wrinkles along the entire shell length are observed.

4 Parametric analysis - "dynamic plastic" and "dynamic progressive" buckling

In addition to the impact velocity, the major parameters, which govern the speed of the development of a single wrinkle, are those related to the inertia properties of a shell defined by (ρh), bending rigidity E_h and ratio σ_0/ρ according to the model described by Eq. (5) - (24).

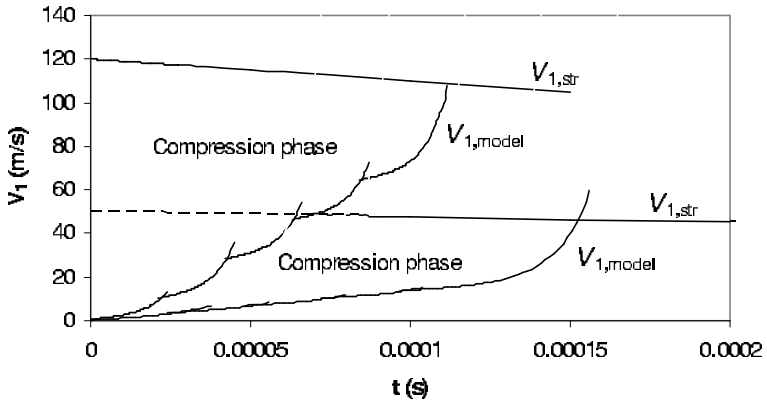
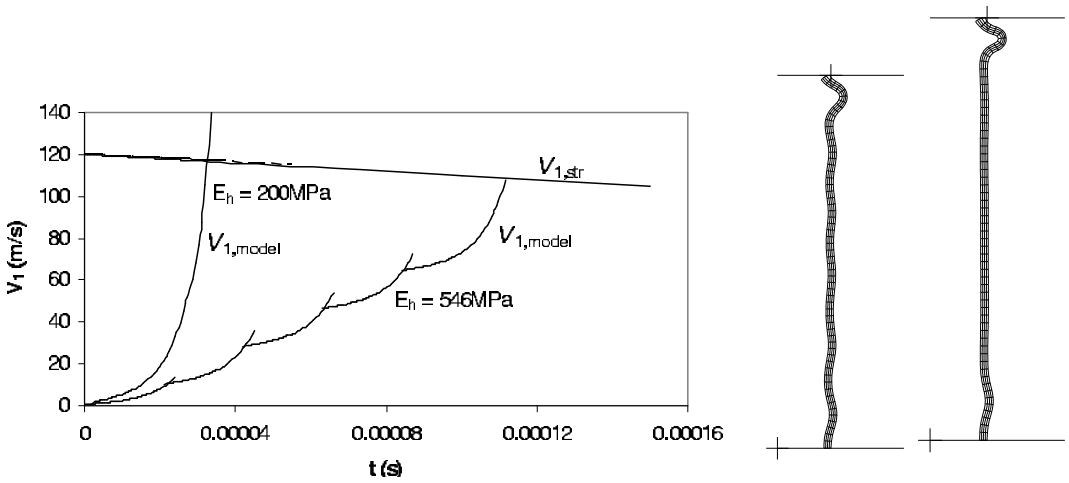


Figure 8: Compression phases in an aluminium alloy shell with $D = 25.4$ mm, $h = 1.65$ mm, $\sigma_0 = 295$ MPa, $E_h = 546$ MPa, $V_0 = 50$ m/s and $V_0 = 120$ m/s predicted by the model for $T_0 = 3.1$ kJ.

Several examples for the duration of the compression phase, which is related to the possibility for the development of buckling within a sustained axial plastic flow and predicted by the model, are shown in Fig. 8-12 for different shell characteristics and loading parameters. The compression phases for aluminium alloy shells subjected to axial impacts with 50 m/s and 120 m/s are shown in Fig. 8. One can see that the compression phase lasts longer for the lower impact velocity. The larger overstress, caused by the higher impact velocity (Eq. (1)) initiate more rapid development of wrinkles with larger magnitudes. For example, wrinkles with magnitudes 0.32 mm, 0.42 mm and 0.65 mm develop under axial impacts with 50 m/s, 75 m/s and 120 m/sec, respectively. That is why, the wrinkles, which develop within a sustained axial plastic flow in aluminium alloy shells become more visible for impacts with higher initial velocities.

An impact with sufficiently high initial velocity can cause a rapid development of the wrinkle near to the proximal end of a shell, which is consistent with the increased initial rotational velocity defined by Eq. (18) for the discrete model. However, this kind of response does not usually occur experimentally since a considerable increase of the shell thickness occurs leading eventually to a "mushrooming" effect [19]. Even no visible mushrooming effect occurs, the increased shell thickness leads to wrinkles with larger wave lengths, which has an implication on the initial condition (18) decreasing the initial rotational velocity. Thus, if a given impact velocity causes "dynamic plastic" buckling of a shell, impacts with even higher initial velocities initiate the same buckling mode (Fig. 8). Due to this reason, the threshold impact velocity for the development of buckling within a sustained axial plastic flow in aluminium alloy shells with particular geometry can be also considered as a lower bound to the impact velocity causing this buckling mode.

The influence of the bending rigidity determined by the hardening modulus, E_h, is shown in Fig. 9 for shells subjected to identical axial impact loadings. The smaller hardening modulus



(a) (b) (c)

Figure 9: (a) Compression phases in an aluminium alloy shell with $D = 25.4$ mm, $h = 1.65$ mm, $\sigma_0 = 295$ MPa, $V_0 = 120$ m/s and $G_0 = 0.4$ kg for different hardening moduli predicted by the model. (b,c) Buckling shapes at $t = 0.14$ ms for $E_h = 546$ MPa and $E_h = 200$ MPa, respectively.

($E_h = 200$ MPa) not only decreases the bending rigidity but also decreases the speed of the plastic stress waves travelling along a shell. Consequently, the radial inertia cannot support the unbuckled shape long enough, so that a rapid growth of the radial displacements, $w = l\psi/2$ occurs leading to the rapid termination of the compression phase as shown in Fig. 9(a) and to the development of a local wrinkle. The initial buckling patterns corresponding to shells made from aluminium alloys with different material hardening characteristics are shown in Fig. 9(b,c). One can distinguish a local wrinkle developed in a shell with the lower strain hardening while wrinkles along the entire shell length are observed in the shell with the higher hardening modulus.

The next examples present the compression phases that can occur in steel shells (any strain rate effects are neglected). A decrease of the ratio σ_0/ϱ leads to a decrease of the impact velocity that might potentially cause buckling within a sustained axial plastic flow depending on the inertia of the shell wall and hardening modulus. The minimum impact velocity, which can cause an instantaneous plastic stresses in a circular shell made from a material with $\sigma_0 = 150$ MPa and $\rho = 7800$ kg/m^3 is 4.4 m/s. It is evident in Fig. 10 that the compression phase for the 10 m/s impact lasts long enough to ensure the development of buckling within a sustained axial plastic flow.

However, in contrast to the response of the aluminium alloy shells discussed previously, the increase of the impact velocity to 30 m/s alters the response of a shell qualitatively. The duration of the compression phase decreases significantly due to the larger initial rotational

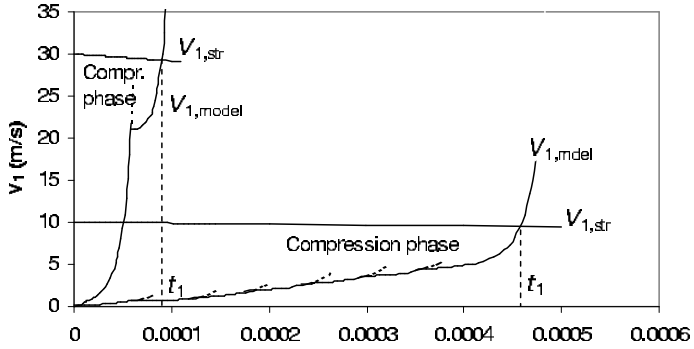


Figure 10: Compression phases in a steel shell with $D = 25.4$ mm, $h = 0.8$ mm, $\sigma_0 = 150$ MPa, $E_h = 100$ MPa for $V_0 = 10$ m/s and $V_0 = 30$ m/s predicted by the model for $T_0 = 2.3$ kJ.

velocity determined by Eq. (18) and a local wrinkle develops near to the proximal end of the shell. The initial and final buckling patterns corresponding to both loading conditions are shown in Fig. 11. Similarly to the response of aluminium alloy shells, a suitable variation of the strain hardening modulus can lead to buckling within a sustained plastic flow as shown in Fig. 12(a) for a shell with $E_h = 400$ MPa.

Thus, the impact velocity is not the only factor causing buckling within a sustained axial plastic flow provided that $V_0 > V_{0,plastic}$. Depending on the geometrical and material characteristics of a shell, this buckling mode can develop for high as well as for relatively low impact velocities (Fig. 12(b)).

The above analysis suggests that $V_0 > V_{0,plastic}$ is a necessary condition for the development of buckling within a sustained axial plastic flow and it is a function of the material properties of a shell. The sufficient condition is determined by the predicted velocity at the end of the compression phase at $t = t_1$ and can be formulated as

$$V_{1,str}(t_1) > V_{1,model}(t_1), t < t_1. \tag{25}$$

It is evident that dynamic buckling within a sustained axial plastic flow ("dynamic plastic" buckling) can be observed only for particular combinations between the shell characteristics and material properties. For certain parameters this buckling mode could never occur regardless of the impact velocity, that is why, localized buckling is more commonly observed in the tests on axial impact loadings of shells. Furthermore, strain rate effects, which are characteristic of many types of steel and other ductile materials, cause more rapid strain localization [10], therefore, so called "progressive" buckling develops even for high velocity impacts. Perhaps, certain aluminium alloys are the most appropriate ductile materials for an analysis of dynamic buckling within a sustained axial plastic flow. Potentially, shells made from materials with low yield stress and high density may develop so called "dynamic plastic" buckling as a response to

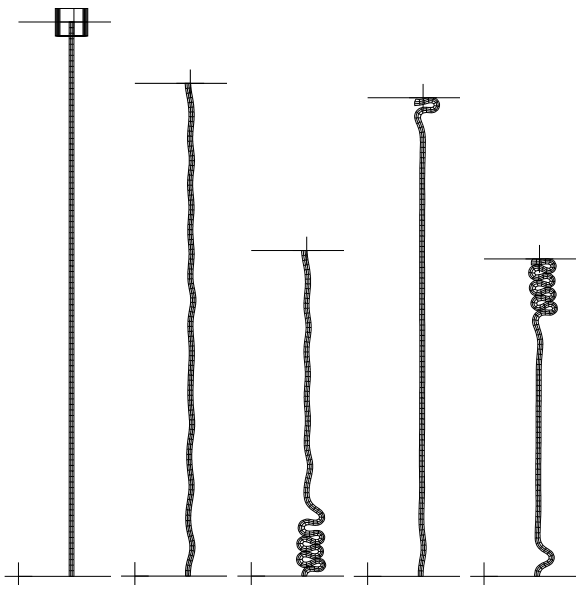


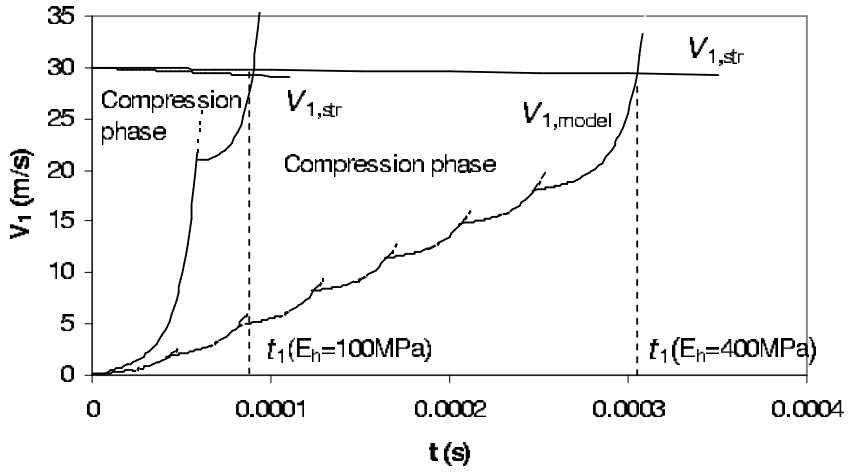
Figure 11: Buckling shapes of steel shells with $D = 25.4$ mm, $h = 0.8$ mm, $\sigma_0 = 150$ MPa, $E_h = 100$ MPa, $T_0 = 2.3$ kJ. (a) Undeformed; (b,c) $V_0 = 10$ m/s - initial an final buckling shape; (d,e) $V_0 = 30$ m/s - initial and final buckling shape.

relatively low impact velocity due to the low values of $V_{0,plastic}$. For example, shells made from a steel with these characteristics and a negligible strain rate effect can exhibit "dynamic plastic" buckling for low impact velocity (Fig. 11) while shells made from some aluminium alloys require considerably higher impact velocity to initiate this particular buckling mode (Fig. 1).

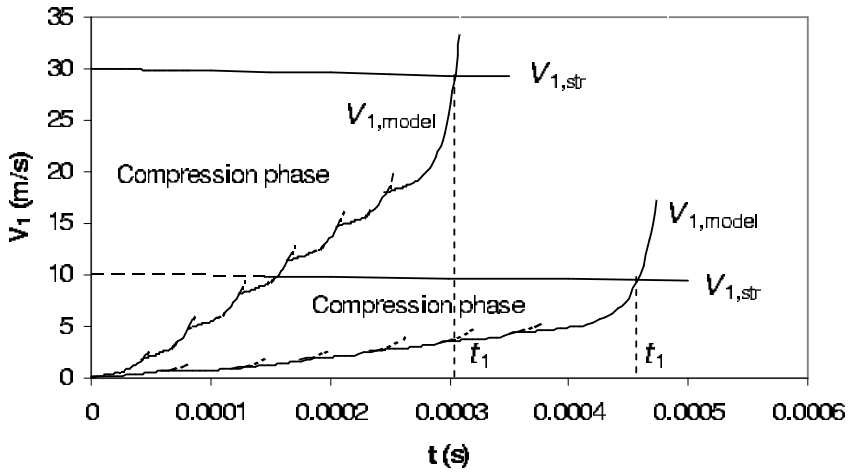
5 Conclusions

The phenomena of "dynamic plastic" buckling (when the entire length of a cylindrical shell wrinkles before the development of large radial displacements) and "dynamic progressive" buckling (when the folds in a cylindrical shell form sequentially) are analysed from the viewpoint of stress wave propagation resulting from an axial impact. It is shown that the particular impact velocity, which instantaneously causes stresses exceeding the elastic limit of the material at the proximal end of a shell, and therefore can cause an initial instability pattern within a sustained axial plastic flow, depends on the material properties, so that $V_0 > V_{0,plastic}$ is referred to as a necessary condition.

A phenomenological approach is used to estimate the impact velocity, which causes "dynamic plastic" buckling of a circular shell and it is associated with the sufficient condition for the



(a)



(b)

Figure 12: Compression phases in a steel shell with $D = 25.4$ mm, $h = 0.8$ mm and $\sigma_0 = 150$ MPa predicted by the model for $T_0 = 2.3$ kJ. (a) $V_0 = 30$ m/s for a shell having different hardening moduli; (b) $V_0 = 30$ m/s for a shell having $E_h = 400$ MPa and $V_0 = 10$ m/s for a shell having $E_h = 100$ MPa.

development of buckling within the sustained axial plastic flow for a particular shell. The analysis reveals that "dynamic plastic" buckling can develop for relatively low impact velocity, too provided that a shell has certain inertia characteristics. The latter conclusion is in contrast with the established perception that a high impact velocity is a necessary condition for the initial shell instability within a sustained axial plastic flow when "dynamic plastic" buckling of elastic-plastic shell can be observed experimentally during the impact tests.

Furthermore, the sufficient condition given by Eq. (25) cannot be generally regarded as a lower bound to the impact velocity that causes "dynamic plastic" buckling of a shell. It is shown that a shell, which responds by buckling within a sustained axial plastic flow to an impact with a certain initial velocity, can respond by a localized buckling to a higher impact velocity. Therefore, more precise definitions for the two types of axisymmetric buckling of circular cylindrical shells that may result from an axial impact can be given as a *localized buckling* (progressive) and *buckling within a sustained axial plastic flow* (plastic). Both buckling modes can occur plastically under axial dynamic loadings. If the necessary condition given by Eq. (25) is satisfied the entire length of a cylindrical shell can wrinkle before the development of large radial displacements.

Acknowledgments – The support from the Bulgarian National Research Fund through contract TH-1103/01 is greatly acknowledged.

References

[1] J.N. Goodier. Dynamic plastic buckling, In: Proceedings of the Int Conf on Dynamic Stability of Structures, Ed. G. Herrmann, Pergamon, New York, 189–211, 1967.

[2] K. Murase and N. Jones. The variation of modes in the dynamic axial plastic buckling of circular tubes, In: N.K. Gupta (Ed.), Plasticity and Impact Mechanics, Wiley Eastern Limited, New Delhi, pp. 222–237, 1993.

[3] Li Ming, Wang Ren and Han Mingbao. An experimental investigation of the dynamic axial buckling of cylindrical shells using a Kolsky bar, Acta Mech. Sinica, 10:260–266, 1993.

[4] T. Kurokawa, T. Sasaki, H. Suzuki and Y. Iamada. Axisymmetric collapse of circular tubes due to longitudinal impact, In: Proceedings of the Sino-Japanese Symposium on Deformation and Fracture of Solids, Huangshang, China, pp. 9–16, 1997.

[5] Wang Ren, Han Mingbao, Huang Zhuping and Yan Qingchun. An experimental study on the dynamic axial plastic buckling of a cylindrical shell, Int J Impact Eng, 1:249–56, 1983.

[6] W. Abramowicz and N. Jones. Transition from initial global bending to progressive buckling of tubes loaded statically and dynamically, Int J Impact Eng, 19(5-6):415–437, 1997.

[7] S.S. Hsu and N. Jones. Dynamic axial crushing of aluminium alloy 6063-T6 circular tubes, Latin American J Solids and Structures, 1(3):277–296, 2004.

[8] N.K. Gupta and S.K. Gupta. Effect of annealing, size and cut-outs on axial collapse behaviour of circular tubes, Int J Mech Sci, 35(7):597–613, 1993.

[9] D. Karagiozova, M. Alves and N. Jones. Inertia effects in axisymmetrically deformed cylindrical shells under axial impact, Int J Impact Eng, 24:1083-1115, 2000.

[10] D. Karagiozova and N. Jones. Influence of stress waves on the dynamic plastic and dynamic progressive buckling of cylindrical shells under axial impact, Int J Solids Struct, 38:6723-6749, 2001.

[11] D. Karagiozova and N. Jones. On dynamic buckling phenomena in axially loaded elastic-plastic cylindrical shells, Int J Non-Linear Mech, 37:1223–1238, 2002.

[12] D. Karagiozova and M. Alves. Transition from progressive buckling to global bending of circular shells under axial impact - Part I: Experimental and numerical observations, Int J Solids and Structures, 41:1565–1580, 2004.

[13] D. Karagiozova and M. Alves. Transition from progressive buckling to global bending of circular shells under axial impact - Part II: Theoretical analysis, Int J Solids and Structures, 41:1581–1604, 2004.

[14] D. Karagiozova. On the mechanics of the global bending collapse of circular tubes under dynamic axial load - Part I: Structural models, Submitted to Int J Impact Eng, 2004.

[15] D. Karagiozova and N. Jones. On the mechanics of the global bending collapse of circular tubes under dynamic axial load - Part II: Dynamic buckling transition criterion, Submitted to Int J Impact Eng, 2004.

[16] N. Jones. Structural Impact.Cambridge University Press, Cambridge, 1989.

[17] A.L. Florence and J.N. Goodier. Dynamic plastic buckling of cylindrical shells in sustained plastic flow, J Appl Mech 35:80–86, 1968.

[18] W. Abramowicz and N. Jones. Dynamic axial crushing of circular tubes, Int J Impact Eng, 2:263–281, 1984.

[19] B. Wang and G. Lu. Mushrooming of circular tubes under dynamic axial loading, Thin-Walled Structures, 40(2):167–182, 2002.